Journal of Organometallic Chemistry 880 (2019) 39–46

Contents lists available at ScienceDirect

Journal of Organometallic Chemistry

journal homepage: www.elsevier.com/locate/jorganchem

Oxidation kinetics of ferrocene derivatives with dibenzoyl peroxide

Joshua M. Halstead [a], Refaat Abu-Saleh [a], Steven M. Schildcrout [b, *], John Masnovi [a, 1]

[a] Department of Chemistry, Cleveland State University, Cleveland, OH, 44115, USA
[b] Department of Chemistry, Youngstown State University, Youngstown, OH, 44555, USA

ARTICLE INFO

Article history:
Received 27 September 2018
Received in revised form
18 October 2018
Accepted 25 October 2018
Available online 27 October 2018

Keywords:
Ferrocene
Peroxide
Kinetics
Single-electron transfer
Marcus theory
B3LYP calculation

ABSTRACT

Chemical oxidation of ferrocene and related derivatives by dibenzoyl peroxide in acetonitrile solution produces ferrocenium and benzoic acid after acidification. The rate law is first order in oxidant and in reductant. Steric effects and activation parameters are consistent with a rate-controlling outer-sphere single-electron transfer (ET) step, and reorganization energies are obtained using Marcus theory with B3LYP calculations. Energetics, optimized structures, and solvent effects indicate that rate is affected more by anion than cation solvation and that oxidation of decamethylferrocene by 3-chloroperoxybenzoic acid does not occur by ET.

1. Introduction

Peroxide oxidations of iron compounds are important and ubiquitous processes. One example is Fenton's reagent. This system, which combines catalytic ferrous iron with hydroperoxides, has attracted considerable attention for its capability to destroy environmentally persistent halogenated organic compounds [1]. The reaction is believed to involve oxidation of Fe(II) to Fe(III) with production of hydroxyl radicals as secondary oxidants [2]. These reactions are complex, with many side reactions and byproducts, which makes them difficult to study [3]. Turnover numbers are also relatively low for reasons which are poorly understood. Greater knowledge of the Fenton mechanism could lead to the design of more efficient catalysts for their use in green chemistry to destroy environmental pollutants.

Peroxidases [4] and cytochrome *c* systems [5] contain heme iron and catalyze the oxidation of organic substrates with hydrogen peroxide. Oxyferryl and other intermediates are believed to mediate these processes [6]. The enzymes and their mimics are inherently unstable, being prone to inactivation during normal turnover, which is the major limitation to their commercial application [7]. Additional work is needed to understand the mechanisms regarding the activity and peroxide-driven inactivation of such enzymes to improve their properties, such as by protein engineering.

Ferrocenes provide simpler models to investigate oxidations of Fe(II). Reversible single electron transfers involving these compounds are well-known using electrochemical methods where an electrode serves as the electron acceptor. These processes occur at lower oxidation potentials in the presence of more electron-donating substituents on the cyclopentadienyl rings. However, the kinetics of homogeneous chemical oxidations of ferrocenes by electron transfer have not been well explored [8]. In ferrocene, straightforward aromatic substitution reactions are only irregularly successful even though ferrocene possesses aromatic stability [9]. Thus, ferrocene cannot be nitrated directly by nitronium-producing systems [10]. The reason for this behavior is unclear, but it may be related to the ease of oxidation of ferrocenes by electron transfer and the further reactivity of the ferrocenium ions so produced [11]. Electron transfer has been shown to be a viable mechanism for nitration of other aromatics as well as nitroaromatic compounds with low oxidation potentials [12,13].

An oxidative addition mechanism for reactions of ferrocenes must also be considered. Many chelation complexes which contain transition metals in low coordination and oxidation states react in this fashion [14], most notably square planar Pt(II). For example, dibenzoyl peroxide (DBP) [15] and peroxy acids [16] react through

* Corresponding author.
E-mail address: smschildcrout@ysu.edu (S.M. Schildcrout).
[1] Deceased 10 September 2018. His coauthors dedicate this paper to his memory.

https://doi.org/10.1016/j.jorganchem.2018.10.022
0022-328X/

oxidative addition of the O-O bond to a *trans*-Pt(II) moiety. Furthermore, second-order rates and large negative entropies of activation were determined for the addition of DBP to diarylplatinum(II) complexes [17]. Additions may be distinguished from electron transfers by stereoelectronic effects. Sterics, for example, should play a smaller role in electron transfer which can occur over a larger separation between reactants by an outer-sphere mechanism [18], and electron donation from the ligands would be more important. Conversely, steric effects should greatly influence oxidative addition where two new bonds to the metal are formed and the electron count would increase to 20. In this case greater electron donation from the ligands to the metal might not be very activating as iron would expand its valence beyond the preferred count of 18.

Given the importance of understanding electron-transfer in chemical and biological reactions [19], we studied the oxidation of ferrocene (Fc), decamethylferrocene (DMFc), and related derivatives with DBP to investigate the underlying mechanisms for these chemical processes. To test whether the DBP interpretation might extend to other organic peroxides, the reaction of DMFc with 3-chloroperoxybenzoic acid (mCPBA) was examined also. B3LYP density functional calculations were performed for the reactants and products to provide energetics [20], which were correlated with experimental results. The effect of various solvents on reaction rate was also investigated.

2. Material and methods

Stock solutions of Fc (Aldrich), DMFc, (Aldrich), ethylferrocene (EtFc, Aldrich), acetylferrocene (AcFc, prepared according to [21], m.p. 83.0–86.0 °C), and bromoferrocene (BrFc, prepared according to [22], m.p. 30.0–32.0 °C) were made by dissolving the requisite compounds in reagent grade acetonitrile (Aldrich). The oxidants DBP (Aldrich), and mCPBA (Aldrich) were also dissolved in acetonitrile. Just prior to the reactions of BrFc, Fc, and AcFc, 1 μL of trifluoromethanesulfonic acid (TFA, Aldrich) was added. TFA addition was found not to affect the kinetics of the oxidations but helped stabilized and solubilize the product salts. Distilled water (10 μL/3 mL solution) was added to all reactions for the same purpose. The absorptions of the ferrocenium cations (Fig. 1a) were confirmed by comparison with authentic samples of their trinitromethide salts [23] obtained by single-electron transfer oxidation of the ferrocenes using tetranitromethane [24]. The reactions were rapid, which required the use of low reactant concentrations and resulted in small absorbance changes. Therefore, these ferrocenes were monitored at five selected wavelengths between 300 and 800 nm where the changes in absorbance were largest. Reaction rates did not depend on the wavelength used. Reaction of AcFc with DBP was found to be too slow to obtain accurate rate measurements even at the limit of solubility.

The reaction rates were determined to be first order with respect to ferrocene and peroxide, and second order overall. Due to the instability of the ferrocenium ions in the presence of excess peroxide, reactions were initiated under pseudo-first order conditions using a minimum 5-fold stoichiometric excess of ferrocene derivative and the kinetics determined when the ferrocene concentrations were at least 10 times that of the peroxide. The following series of reactions were performed in triplicate: (1) 3 mL of ferrocene solution ranging in concentration from 10 to 18 mM,1 μL of TFA, and 6 μL of 60 mM DBP solution, (2) 3 mL of DMFc solution ranging in concentration from 0.04 to 0.12 mM and 2 μL of 6 mM DBP solution, (3) 3 mL EtFc solution ranging in concentration from 2 to 6 mM and 10 μL of 60 mM DBP solution, (4) 3 mL of BrFc solution ranging in concentration from 30 to 50 mM, 1 μL TFA, and 30 μL of 60 mM DBP solution, and (5) 3 mL of DMFc solution ranging in concentration from 1.6 to 2.4 mM and 2 μL of 60 mM mCPBA solution. Each reaction was conducted in a quartz cuvette using a temperature-controlled Hewlett-Packard HP8452 spectrophotometer. Spectra were measured at 1 s intervals and calculations performed for absorbance changes at 617 nm (Fc and BrFc, as shown in Fig. 1a) or 330 nm (EtFc, DMFc). Each reaction was performed at temperatures ranging from 0 °C to 50 °C. Measurements were stopped when the change in absorbance essentially reached an asymptote as shown for a representative reaction in Fig. 1b.

Product studies were conducted on a larger scale. Titration of the reactions revealed that the stoichiometry of ferrocene:peroxide was 2:1 in every case. Therefore, each ferrocene derivative was allowed to react with DBP at a 2:1 molar ratio for 30 min at 22.0 °C at the following concentrations: (1) 0.100 g of DMFc dissolved in 300 mL of acetonitrile and 0.040 g of DBP dissolved in 10 mL of acetonitrile, (2) 0.100 g of Fc dissolved in 300 mL of acetonitrile, 0.065 g of DBP in 10 mL of acetonitrile, and 1 μL of TFA, (3) 0.100 g of EtFc dissolved in 300 mL of acetonitrile and 0.056 g of DBP in 10 mL of acetonitrile, (4) 0.100 g of BrFc dissolved in 300 mL of acetonitrile, 0.0460 g of DBP in 10 mL of acetonitrile, and 1 μL of TFA. Ferrocenium ions and the residual ferrocenes were assayed spectrophotometrically. The benzoic acid was extracted with aqueous sodium bicarbonate, precipitated by acidification with concentrated HCl, filtered, and dried. The precipitate was characterized by melting point and confirmed by ^{1}H and ^{13}C NMR (400 MHz Bruker Avance NMR) and mass spectrometry (Varian Saturn 2100T GC/MS). Yields were determined gravimetrically and were nearly quantitative based on the amount of ferrocene consumed (Table 1).

The effect of solvent was examined at 20.0 °C using 3 mL of a 0.12 mM DMFc solution created using ethanol, acetone, acetonitrile, or 1,2-dicholoroethane combined with 3 μL of 6 mM DBP solution. mCPBA was also investigated using 3 mL of a 0.24 mM DMFc solution created using the aforementioned solvents combined with 6 μL of 6 mM mCPBA also in the corresponding solvent.

Computations were performed for molecular and ionic geometries and energies in acetonitrile, including ΔG° for electron transfer and the nuclear component of reorganization energy (λ_i). Initial-guess conformations and geometries were obtained by molecular-mechanics energy minimization. All-electron (U)B3LYP/6-31+G* was then used in Gaussian 09 [25] through the Ohio Supercomputer Center [26] to obtain optimized geometries and energies. Unrestricted B3LYP for radicals avoids the excessive spin contamination encountered with the UMP2 method. UB3LYP should also better describe the energetics of these systems than restricted open-shell ROB3LYP since, in a computational study using UB3LYP/m6-31G*, ionization of isolated Fc showed reordering of valence MOs with different configurations for α electrons than for β electrons of Fc^{+} [27]. This is confirmed in the present calculations. The solvent was treated using the polarizable continuum model, solute in a cavity in the solvent reaction field (Gaussian keyword SCRF) [28]. Vibrational analyses verified that optimized geometries were at true potential-energy minima and provided free energies.

3. Results and discussion

3.1. Kinetics

The reactions of ferrocenes (RFc) with DBP afford the corresponding ferrocenium benzoate salts with 2:1 stoichiometry:

$$2\ \mathrm{RFc} + (\mathrm{C_6H_5CO_2})_2 \rightarrow 2\ \mathrm{RFc^{+}}\ \mathrm{C_6H_5CO_2^{-}} \qquad (1)$$

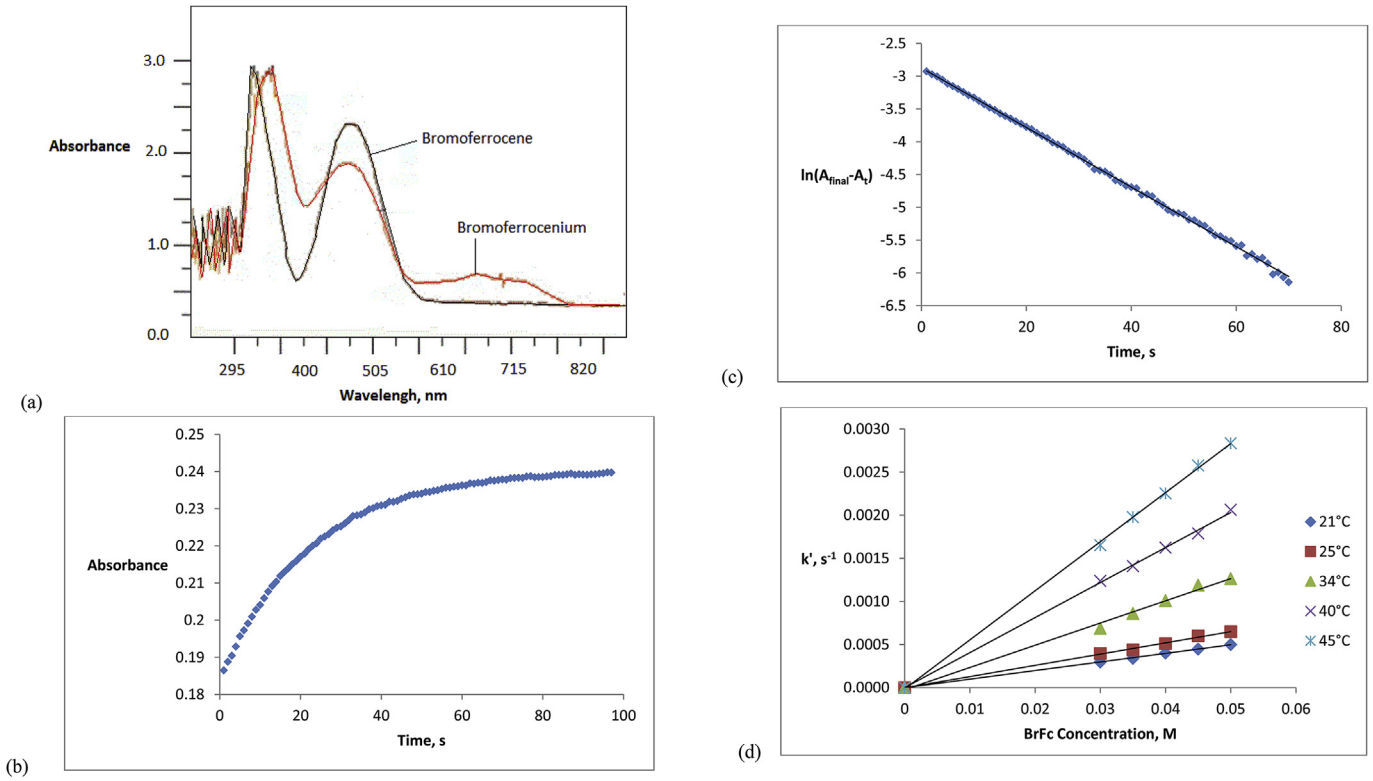

Fig. 1. (a) UV–Vis spectrum before and after reaction of 4.95×10^{-2} M BrFc with 4.9×10^{-4} M DBP ($t = 0$ brown, $t = 1800$ s red); (b) absorbance change at 330 nm and (c) determination of the pseudo-first order rate constant for reaction of 3 mL of 1.2×10^{-4} M DMFc with 2 μL of 6.0×10^{-3} M DBP at 22.5 °C; (d) determination of second-order rate constants k for reactions of BrFc with DBP. (For interpretation of the references to color in this figure legend, the reader is referred to the Web version of this article.)

Table 1
Isolation of benzoic acid from ferrocenes + DBP after 30 min reaction time.

Ferrocene	Benzoic acid formed (%)	Unreacted ferrocene (%)
Fc	72.5	25
EtFc	81.7	17
DMFc	92.2	5
BrFc	69.4	29

All reactions follow second order kinetics

$$d[RFc^+]/dt = k[RFc][peroxide] \quad (2)$$

and were monitored by the growth of ferrocenium absorbances under pseudo-first-order conditions of approximately constant [RFc]. Experimental pseudo-first-order rate constants (k') are determined as least-squares slopes from plots of $\ln(A_{final} - A_t)$ versus time where A is absorbance (Fig. 1c). Second-order rate constants $k = ½\ k'/[RFc]$ are obtained from the slopes of plots of k' versus [RFc] (Fig. 1d), the factor of one-half accounting for the stoichiometry in Equation (1).

The absorptions of Fc^+ and $BrFc^+$ were found to bleach with time, which complicated the analysis. Although ferrocenium cations have been proposed to react with molecular oxygen [29], deaerating the solutions did not stop further reaction of the ferrocenium ions. Independent measurements confirmed the instability of these cations, especially in the presence of peroxide. Addition of a small amount of TFA was found to stabilize the cations on the time scale of the measurements without affecting the reaction rates. The faster reactions of DMFc and EtFc form more stable cations, and therefore did not require stabilization by TFA.

Two mechanistic inferences are noted. First, the ten methyl groups on the pentamethylcyclopentadienyl rings (Cp*) of DMFc do not impede the reaction. To the contrary, DMFc reacts faster with DBP than do any of the other ferrocenes with less bulky substituents. This indicates that intramolecular electron donation by the ligands promotes the reaction more than steric effects might hinder it. This strongly argues for an electron-transfer mechanism occurring over a longer distance, obviating the need for the DBP oxidant to approach the iron center. Second, the observation that the reactions are first-order in ferrocene, but consume ferrocene and DBP in a 2:1 mole ratio, requires a second ferrocene molecule to participate after the rate-limiting step.

3.2. Activation parameters

In order to further explore the nature of the process, activation parameters (Table 2) are estimated (Fig. 2) using the Eyring equation (Equation (3))

$$\frac{\ln k}{T} = \frac{-\Delta H^{\ddagger}}{RT} + \frac{\ln \kappa k_B}{h} + \frac{\Delta S^{\ddagger}}{R} \quad (3)$$

where the transmission factor κ is assigned the value 1, k_B is Boltzmann's constant, h is Planck's constant, R is the gas constant, and T is the absolute temperature. Activation entropies $\Delta S^{\ddagger}$ in Table 2 are consistent with ionization occurring during (or before) the rate-limiting step.

Large negative activation entropies are common for ionizations due to solvent effects [30]. The activation entropy shows a trend where ferrocene derivatives with larger substituents have more negative $\Delta S^{\ddagger}$. This is expected because increasing the molecular radius should result in a larger, more ordered solvent shell [31]. The radius of DMFc (6.00 Å [32]) is the largest, and its entropy is most

Table 2
Rate constants and activation parameters for reactions studied and ΔG° computed for electron transfer.

Reaction	k, $M^{-1}s^{-1}$[a]	$\Delta H^{\ddagger}$, kJ/mol	$\Delta S^{\ddagger}$, J/mol·K	$\Delta G^{\ddagger}$, kJ/mol[a]	ΔG°, kJ/mol[b]
Fc + DBP	0.162	59 ± 1	−60 ± 7	76.7	−8.0
EtFc + DPB	0.345	49.9 ± 0.5	−85 ± 4	75.0	−15.4
DMFc + DBP	269	24.5 ± 0.2	−115 ± 1	58.4	−63.0
DMFc + mCPBA	4.85	61.5 ± 0.5	−24 ± 3	68.0	183.0
BrFc + DBP	0.0100	54.6 ± 0.2	−98 ± 1	83.8	16.3

[a] 22.0 °C.
[b] (U)B3LYP/6-31+G* at 25.0 °C.

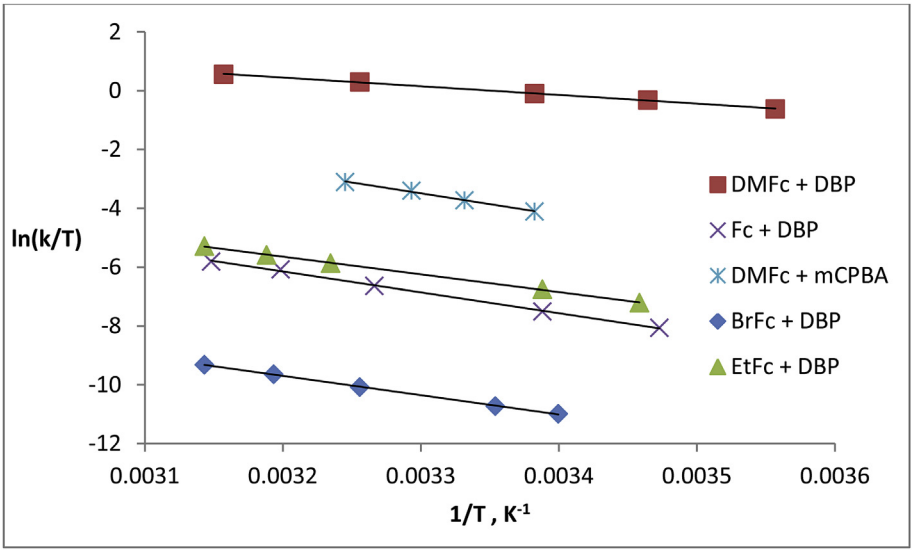

Fig. 2. Eyring plots of Fc derivatives reacting with DBP and mCPBA in acetonitrile.

negative, while Fc has the smallest radius (4.07 Å [32]) and the least negative entropy. Similarly, mCPBA is smaller than DBP, and the activation entropy for reaction of DMFc with mCPBA is more favorable than that with DBP. Such a trend supports an outer-sphere electron transfer mechanism for which solvation is a key step.

The activation enthalpies generally trend in the same direction as entropy, with the lowest (most favorable) $\Delta H^{\ddagger}$ found for reaction of DMFc with DBP, which has the lowest (least favorable) entropy. The fact that DMFc requires the least energy is indicative of electron donation from the ten methyl groups, resulting in a greater reaction rate with a low $\Delta H^{\ddagger}$. The $\Delta H^{\ddagger}$ for reaction of EtFc with DBP is next lowest. BrFc and Fc show a similar $\Delta H^{\ddagger}$ with BrFc being slightly lower. The rates of the latter compounds correlate with the Hammett σ_p constants [33] with $\rho = -3.5$ determined as the slope/2.303 in Fig. 3. Although determined from only ferrocene and its two monosubstituted derivatives, the negative ρ is consistent with facilitation of reaction by electron-releasing substituents and development of positive charge at the reaction center, the Fe atom.

Operation of such an effect is supported also by the observed trend in the yields of benzoic acid, namely DMFc > EtFc > Fc > BrFc (Table 1), so that the ferrocenes with more electron-rich centers react further and faster than their less electron-rich counterparts. This would not be expected so much for an oxidative addition, by which no charge is developed on iron and its electron count actually increases.

The less favorable activation enthalpy for reaction of DMFc with mCPBA compared to DBP likely is due to mCPBA being a weaker oxidant than DBP. The respective electron affinities of DBP and mCPBA are calculated for optimized geometries in acetonitrile as

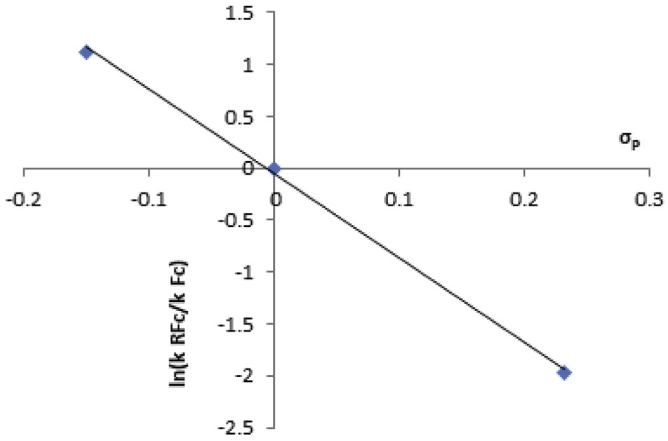

Fig. 3. Hammett plot for reactions of EtFc, Fc, and BrFc with DBP.

5.07 eV and 2.64 eV. These calculations reveal that electron attachment to DBP is effectively dissociative, with the O-O bond distance increasing from 1.433 Å for the neutral molecule to 2.201 Å for the radical anion $DBP^{\bullet-}$ in the optimized structure. This indicates that the latter is essentially a loose complex of benzoate anion and benzoyl radical with small binding energy (15.3 kJ/mol) and spontaneous dissociation ($\Delta G^{o} = -19.8$ kJ/mol) at 298 K. Dialkyl peroxides were reported to undergo dissociative electron capture also [34]. On the other hand, the O-O distance in mCPBA increases from 1.440 Å to just 1.451 Å in the radical anion $mCPBA^{\bullet-}$. The shorter

bond distance implies a stronger O-O bond in the latter anion than in $DBP^{\cdot-}$. Therefore, electron capture by DBP would be irreversible or nearly so, with $DBP^{\cdot-}$ being associated weakly if at all, but this may not be so for $mCPBA^{\cdot-}$. The small electron affinity for mCPBA and the incompatible result (Table 2) that $\Delta G^{\ddagger}$ is much less than the positive ΔG^{o} calculated for electron transfer of DMFc to mCPBA suggest a different, more competitive mechanism for this case. For example, a speculative initial rate-limiting oxidative addition DMFc + mCPBA → $[DMFc\text{-}OH]^{+}$ + $m\text{-}ClC_6H_4CO_2^{-}$ has a calculated $\Delta G^{o} = -83.3$ kJ/mol and would be consistent with the observed second-order rate law. The cation produced in this step has an optimized structure with two nonparallel η^5-Cp* groups sterically accommodating the new Fe^{IV}-O bond (1.972 Å). A fast second step $[DMFc\text{-}OH]^{+}$ + DMFc → 2 $DMFc^{+}$ + OH^{-} would give two Fe(III).

3.3. Solvent effects

Solvent has surprisingly little effect on the rate constant for reaction of DMFc with DBP (Table 3) if it involves an electron transfer. The rates do not correlate monotonically with dielectric constant. Reaction rates rank ethanol > acetonitrile > ethylene chloride > acetone although the largest difference is less than a factor of 3. The effect of substituents (Table 2) is much larger than this. The correlation is better with spectroscopic estimates of solvent polarity as used for Reichardt's E_T and Kosower's Z values (Table 3). These scales were developed using the charge-transfer absorption energies of organic salts, which would include specific solvation effects and not just bulk solvent properties. Here the absorption of a photon promotes a vertical transfer of an electron, which more resembles chemical electron transfer. However, the latter reaction involves electron transfer from polar but uncharged starting materials to form ions rather than the reverse, and it is nonadiabatic. Therefore, the role of solvent may differ between the chemical and photochemical processes, and the analogy should not be expected to be exact.

Furthermore, photoelectron spectroscopy reveals that the highest three occupied molecular orbitals of Fc are principally metal 3d in nature with little ligand character [40]. This means that the charge in ferrocenium should be localized mostly on iron. Since the metal atom is isolated from strong interactions with the solvent by the Cp rings and their substituents, solvation should be relatively ineffective in stabilizing the charge, especially in $DMFc^{+}$. Hence the DMFc/$DMFc^{+}$ redox couple is well-defined and only mildly dependent on solvent [41], consistent with this analysis. Ferrocenes are unusual in that their carbon atoms bear partial negative charge and the central iron some positive charge even in the neutral compounds [42]. Therefore, ionization, depicted in Fig. 4, should decrease the outermost (negative) charge interacting with solvent so that solvent effects may differ from reactions which produce more exposed positive charges such as in carbocations. This interpretation is consistent with the Mulliken partial charges resulting from the (U)B3LYP calculations for all RFc and $RFc^{\cdot+}$.

Consequently, the solvent effects may have more to do with solvation of the anions than the ferrocenium cations. As Mulliken population analysis confirms, the negative charge in $DBP^{\cdot-}$ resides primarily on oxygen, especially the keto O atoms, whereas in the products the negative charge is delocalized over the carboxylate anion fragment. Protic solvents like ethanol strongly solvate anions by hydrogen bonding whereas aprotic solvents like acetone, acetonitrile and ethylene chloride with large dipole moments solvate cations better [32]. Therefore, solvent polarity might be less important since the ferrocenium cations are not well solvated, but the anions would be stabilized by hydrogen bonding. This would result in a larger rate in ethanol than rates in the other solvents which do not correlate with solvent polarity, as observed.

Compared to the DBP reactions, Table 3 shows reaction rates with mCPBA to vary more strongly and with different ordering as solvent is varied, with ethanol giving the slowest rate measured. Since mCPBA has a hydroxyl group but $m\text{-}ClC_6H_4CO_2^{-}$ does not, hydrogen bonding of the former with a protic solvent such as ethanol would stabilize the reacting peroxide relative to the product anion and tend to slow an addition step as hypothesized in Section 3.2. Also electron donor-acceptor complexes have long been known to form between good donors and acceptors [43–45]. Some of these have been shown to be kinetically competent intermediates in a number of bimolecular reactions, such as the Diels-Alder reaction [46]. The formation of such complexes between the ferrocenes and peroxides seems likely considering the polar nature and accepting ability of the ferrocenes. Clearly the effect of solvent in these processes is complex and warrants further study.

3.4. Marcus modelling

To rationalize the effect of Fc substituents on observed oxidation rates, a Marcus-type model is used for the electron transfer step. The total reorganization energy, λ, which is defined as the sum of the nuclear reorganization energy, λ_i, and outer sphere reorganization energy, λ_o, is calculated using the experimentally derived Gibbs activation energy, $\Delta G^{\ddagger}$, and the computationally derived standard Gibbs energy of reaction, ΔG°, using Equation (4) (Table 2) [20].

$$\Delta G^{\ddagger} = \frac{(\Delta G^{0} + \lambda)^{2}}{4\lambda} \tag{4}$$

The λ values for the reaction of ferrocenes with peroxide are typically quite large, in the range of 300–400 kJ/mol, whereas the λ values for the reported inner-sphere electron transfer of hydroquinones with DBP are significantly lower, in the range of 60–80 kJ/mol [47]. Much higher reorganization energies should be expected for outer-sphere compared to inner-sphere electron transfers [48].

Table 3
Effect of solvent on rate constant for DMFc at 20 °C.

Solvent	DMFc + DBP, k (M^{-1} s^{-1})	DMFc + mCPBA, k (M^{-1} s^{-1})	Dielectric Constant[a]	Relative Polarity[b]	$E_T(30)$[b,c]	Z value[d]
Acetone	114	–[e]	20.7	0.355	42.2	65.7
1,2-Dichloroethane	167	10	16.7	0.327	41.9	63.8[f]
Acetonitrile	208	3.3	37.5	0.46	46	71.3
Ethanol	306	2.0	24.3	0.654	51.9	79.6

[a] Ref. [35].
[b] Ref. [36].
[c] Ref. [37].
[d] Ref. [38].
[e] Too slow to measure reliably.
[f] Ref. [39].

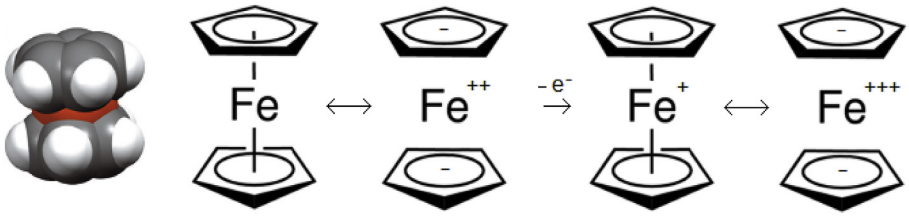

Fig. 4. Structures of ferrocene and ferrocenium ions.

The nuclear reorganization energy is taken to be the sum of the energy differences of each respective ferrocene moiety before and after an electron transfer has taken place in both the initial and final molecular geometries [49]. This idea is further illustrated in Fig. 5, where the sum of the energy difference provides the change in reaction coordinate, defined as λ_i. The overall relationship between λ and ΔG is shown in Fig. 6. Note that the λ_i results are for ferrocene species only and do not include the reorganization energy of the peroxide. Due to the dissociative behavior of DBP, λ_i cannot be accurately modeled using this method. Although mCPBA can form a stable anion and would contribute $\lambda_i = 56.5$ kJ/mol, as discussed above, it seems too weak an electron acceptor to react with ferrocenes by an electron-transfer mechanism at the rate observed.

The calculation of λ_i is shown in Table 4.

Overall, it is observed that the rate of oxidation depends strongly on the modification of the ferrocene derivative. The Gibbs energy of activation for ferrocene moieties with electron-donating substituents is lower than that of unsubstituted ferrocene and ferrocenes modified with electron-withdrawing substituents. Furthermore, the computed λ_i, which can also be considered as the energy required to modify bond angles and bond distances from reactant to product geometries, is found to be only a minor contributor to the overall reorganization energy, consistent with the very small geometry changes upon electron loss by the ferrocenes. The λ_o component is the much more significant part of λ. This is consistent with an outer-sphere single-electron-transfer mechanism, where λ_o would be expected to provide the largest contribution to the activation energy. The λ_o value is also found to be slightly larger in ferrocene derivatives with electron donating substituents and smaller in the case of electron withdrawing. One explanation for this could be that when electron withdrawing substituents are present on ferrocene the Fe atom already possesses more partial positive charge and therefore requires less stabilization from the solvent environment to transition to the cation product. A mechanism for an outer-sphere electron transfer for Fc + DBP is proposed in Equations (5)–(9) and Fig. 7.

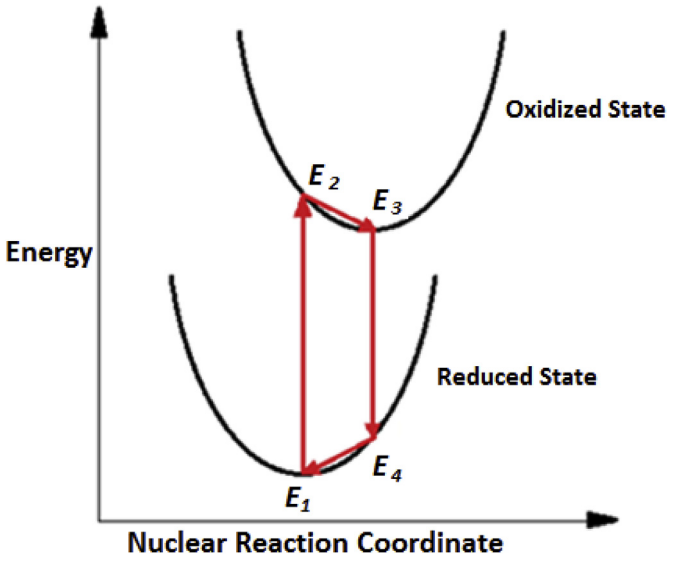

Fig. 5. Schematic potential-energy diagram used to determine λ_i (E_1 and E_3 correspond to optimized minima, and E_2 and E_4 to vertical electron transfer at the geometries E_1 and E_3 respectively).

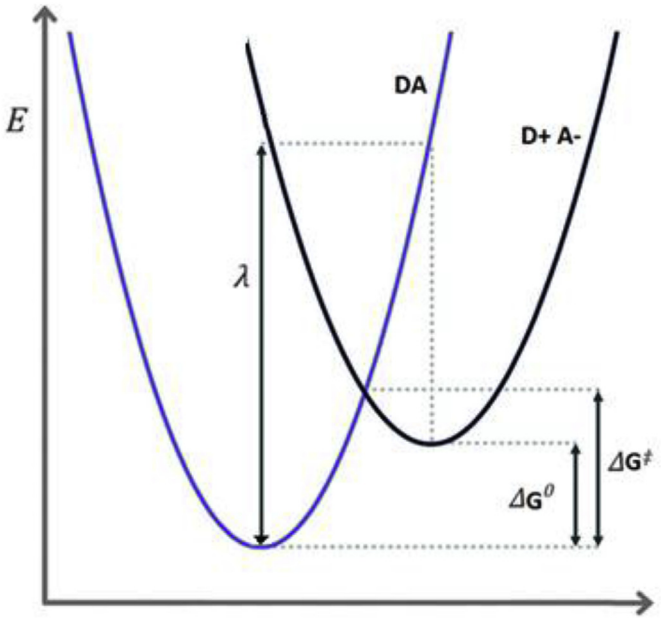

Fig. 6. Schematic energy diagram for endergonic electron transfer between donor D and acceptor A.

Table 4
Determination of λ_i and λ_o for ferrocenes solvated in acetonitrile.

	λ_1, E_h / E_2-E_3	λ_2, E_h / E_4-E_1	λ_i, E_h[a]	λ_i, kJ/mol	λ, kJ/mol	λ_o, kJ/mol[b]
Fc	0.00040	0.00034	0.00075	2.0	323	321
EtFc	0.00059	0.00063	0.00122	3.2	330	327
DMFc	0.00148	0.00128	0.00275	7.2	348	341
BrFc	0.00099	0.00094	0.00193	5.1	302	297

[a] $\lambda_i = \lambda_1 + \lambda_2$.
[b] $\lambda_o = \lambda - \lambda_i$.

$$Fc + (C_6H_5CO_2)_2 = Fc/(C_6H_5CO_2)_2 \text{ fast} \quad (5)$$

$$Fc/(C_6H_5CO_2)_2 \rightarrow Fc^{+} + (C_6H_5CO_2)_2{\cdot}^{-} \text{ slow} \quad (6)$$

$$(C_6H_5CO_2)_2{\cdot}^{-} \rightarrow C_6H_5CO_2^{-} + C_6H_5CO_2{\cdot} \text{ fast} \quad (7)$$

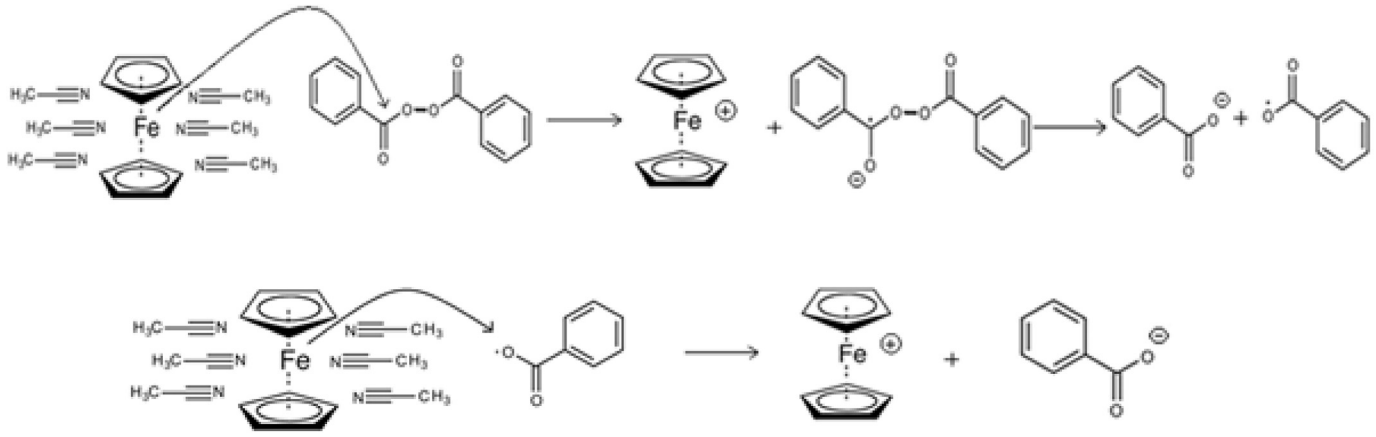

Fig. 7. Proposed outer-sphere electron-transfer mechanism for the oxidation of ferrocene by DBP.

$$Fc + C_6H_5CO_2\cdot \rightarrow Fc^{\cdot+} + C_6H_5CO_2^- \text{ fast} \quad (8)$$

$$2Fc + (C_6H_5CO_2)_2 \rightarrow 2\ Fc^{\cdot+}\ C_6H_5CO_2^- \text{ net} \quad (9)$$

In the above model, the coordination number of the iron center is unchanged, and its oxidation number increases by one. During the first step (Equation (5)), the peroxide approaches the ferrocene molecule to form a weakly coupled complex. The solvent shell surrounding the reactants then assumes the correct geometry and polarization state to facilitate an electron jump, with the peroxide molecule accepting the electron from the iron center of ferrocene to become a radical anion. This is the rate-limiting step (Equation (6)). The O-O bond of the radical anion quickly breaks, forming a benzoyloxy radical and a benzoate anion (Equation (7)), precluding reversal of Equation (6). The radical then interacts with a second ferrocene moiety, which also transfers an electron in a fast step (Equation (8)) completing the observed 2:1 stoichiometry (Equation (9)). Finally, benzoate will metathesize with triflate for reactions performed in the presence of TFA or protonate by the addition of HCl during workup. In these outer-sphere processes, electron donating substituents should promote the reaction, and electron withdrawing substituents should inhibit it. This would also be the case for other mechanisms, such as oxidative addition, but if oxidative addition were taking place significant steric effects would be expected, especially for DMFc, unless geometric changes mitigate them. In this study, electron densities are found to be more important than steric effects, supporting outer-sphere electron transfer to DBP as described by the Marcus model.

4. Conclusions

The reactions of RFc + DBP or mCPBA are characterized by positive activation enthalpy and very negative activation entropy, as expected. The overall trend for DBP is that RFc with electron-donating substituents react much faster, with a lower energy barrier, than unmodified ferrocene, or derivatives with electron withdrawing substituents. The λ_o parameter was found to be inversely related to $\Delta G^{\ddagger}$ indicating that molecules closer in geometry to the product state require less solvent stabilization to facilitate the electron transfer. The computational study provides insight into λ_i which is compared and correlated with the experimental results. It is found that for DBP as oxidant, λ_i is the minor component of the reorganization energy with λ_o the major one. This is consistent with an outer-sphere electron transfer model where ferrocene retains its full coordination shell, and a direct electron transfer from the reductant to the oxidant takes place with no new bonding of ligands that would require kinetically inhibiting geometry changes in the ferrocene. In this type of process solvent polarization is the rate-limiting step and provides the primary component of the activation energy. Furthermore, $\Delta S^{\ddagger}$ correlates with the solvated molecular size of reactants in the expected manner, further highlighting the importance of the solvent for this process. Additionally, no steric hindrance is observed during the oxidation of even the most bulky ferrocene derivatives. Thus, a predominantly outer-sphere electron-transfer mechanism for the oxidation of ferrocenes by DBP is proposed. The rate-limiting step includes an energetically favored dissociative electron capture by DBP, which is not available to mCPBA. Further studies of ferrocene oxidation by peroxides other than DBP are needed.

Acknowledgements

The authors thank the Ohio Supercomputing Center for a grant of computer time. This research did not receive any specific grant from funding agencies in the public, commercial, or not-for-profit sectors.

Appendix A. Supplementary data

Supplementary computational data to this article can be found online at https://doi.org/10.1016/j.jorganchem.2018.10.022.

References

[1] J. Casado, J. Fornaguera, M. Galan, Environ. Sci. Technol. 39 (2005) 1843–1847.
[2] F. Haber, R. Willstätter, Ber. Dtsch. Chem. Ges. 64 (1931) 2844–2856.
[3] C. Walling, Acc. Chem. Res. 8 (1975) 125–131.
[4] I.S. Isaac, J.H. Dawson, Essays Biochem. 34 (1999) 51–69.
[5] M. Carney, J. Lesniak, J. Pladziewicz, J. Am. Chem. Soc. 106 (1984) 2565–2569.
[6] R. Diederix, M. Ubbink, G. Canters, Eur. J. Biochem. 268 (2001) 4207–4216.
[7] R. Sheldon, Nature 399 (1999) 636–637.
[8] J. Frew, M. Harmer, H. Hills, S. Libor, J. Electroanal. Chem. 201 (1986) 1–10.
[9] R. Monson, Advanced Organic Synthesis, Academic Press, Cambridge, 1975.
[10] G. Cerichelli, B. Floris, G. Illuminati, G. Ortaggi, J. Org. Chem. 39 (1974) 3948–3955.
[11] J. Pladziewicz, J. Espenson, J. Am. Chem. Soc. 95 (1973) 56–63.
[12] J. Masnovi, R. Krafcik, R. Baker, R. Towns, J. Phys. Chem. 94 (1990) 2010–2013.
[13] J. Masnovi, S. Sankararaman, J. Kochi, J. Am. Chem. Soc. 111 (1989) 2263–2276.
[14] I. Bauer, H. Knölker, Iron Complexes in Organic Chemistry, Wiley, Hoboken, 2008.
[15] A. Canty, M. Denney, G. Koten, B. Skelton, A. White, Organometallics 23 (2004) 5432–5439.
[16] K. Pellarin, M. McCready, R. Puddephatt, Dalton Trans. 42 (2013) 10444–10453.
[17] M. Rasidi, M. Nabavizadeh, R. Hakimelahi, S. Jamali, J. Chem. Soc., Dalton Trans. (2001) 3430–3434.

[18] R. Marcus, J. Chem. Phys. 24 (1956) 966–978.
[19] H. Heitele, Angew. Chem. Int. Ed. 32 (1993) 359–377.
[20] R. Marcus, N. Sutin, Biochim. Biophys. Acta 811 (1985) 265–322.
[21] P. Graham, R. Lindsey, G. Parshall, M. Peterson, G. Whitman, J. Am. Chem. Soc. 79 (1957) 3416.
[22] R. Fish, M. Rosenblum, J. Org. Chem. 30 (1965) 1253–1254.
[23] R. Abu-Saleh, Ph.D. Dissertation, Cleveland State University, Cleveland, OH, 2007.
[24] J.M. Masnovi, J. Kochi, Recl. Trav. Chim. Pays-Bas 105 (1986) 286–295.
[25] M.J. Frisch, G.W. Trucks, H.B. Schlegel, G.E. Scuseria, M.A. Robb, J.R. Cheeseman, G. Scalmani, V. Barone, B. Mennucci, G.A. Petersson, H. Nakatsuji, M. Caricato, X. Li, H.P. Hratchian, A.F. Izmaylov, J. Bloino, G. Zheng, J.L. Sonnenberg, M. Hada, M. Ehara, K. Toyota, R. Fukuda, J. Hasegawa, M. Ishida, T. Nakajima, Y. Honda, O. Kitao, H. Nakai, T. Vreven, J.A. Montgomery Jr., J.E. Peralta, F. Ogliaro, M. Bearpark, J.J. Heyd, E. Brothers, K.N. Kudin, V.N. Staroverov, T. Keith, R. Kobayashi, J. Normand, K. Raghavachari, A. Rendell, J.C. Burant, S.S. Iyengar, J. Tomasi, M. Cossi, N. Rega, J.M. Millam, M. Klene, J.E. Knox, J.B. Cross, V. Bakken, C. Adamo, J. Jaramillo, R. Gomperts, R.E. Stratmann, O. Yazyev, A.J. Austin, R. Cammi, C. Pomelli, J.W. Ochterski, R.L. Martin, K. Morokuma, V.G. Zakrzewski, G.A. Voth, P. Salvador, J.J. Dannenberg, S. Dapprich, A.D. Daniels, O. Farkas, J.B. Foresman, J.V. Ortiz, J. Cioslowski, D.J. Fox, Gaussian 09, Revision E.01, Gaussian, Inc., Wallingford CT, 2013.
[26] http://osc.edu/ark:19495/hpc0cvqn.
[27] F. Wang, S. Islam, 2015, arXiv.org/abs/1509.05122.
[28] J. Tomasi, B. Mennucci, R. Cammi, Chem. Rev. 105 (2005) 2999–3093.
[29] G. Zotti, G. Schiavon, S. Zecchin, D. Favretto, J. Electroanal. Chem. 456 (1998) 217.
[30] R.G. Pearson, J. Chem. Phys. 20 (1952) 1478–1481.
[31] R. Lichtenthaler, D. Abrams, J. Prausnitz, Can. J. Chem. 51 (1973) 3071–3080.
[32] A. Clegg, N. Rees, O. Klymenko, B. Coles, R. Compton, J. Electroanal. Chem. 580 (2005) 78–86.
[33] D.H. McDaniel, H.C. Brown, J. Org. Chem. 23 (1958) 420–427.
[34] R. Donkers, F. Maran, D. Wayner, M. Workentin, J. Am. Chem. Soc. 121 (1999) 7239–7248.
[35] Honeywell, Dielectric Constant Table, Company Report, 2011 available at: https://www.honeywellprocess.com/library/marketing/tech-specs/Dielectric%20Constant%20Table.pdf.
[36] C. Reichardt, Angew. Chem. Int. Ed. 18 (1979) 98–110.
[37] C. Reichardt, Solvents and Solvent Effects in Organic Chemistry, third ed., Wiley-VCH Publishers, 2003.
[38] E. Kosower, J. Am. Chem. Soc. 80 (1958) 3253–3260.
[39] A. Ohki, K. Tsukada, S. Maeda, M. Takagi, Microchim. Acta 106 (1992) 267–276.
[40] M. Thompson, P. Djurovich, S. Barlow, S. Marder, Comprehensive Organometal. Chem. III 12 (2007) 101–194.
[41] M. Malischewski, M. Adelhardt, J. Sutter, K. Meyer, K. Seppelt, Science 353 (2016) 678–682.
[42] T. Lowery, K. Richardson, Mechanism and Theory in Organic Chemistry, third ed., Harper Collins Publishers, 1987, p. 183.
[43] M. Kloetzel, Diels-alder reaction with maleic anhydride, in: R. Adams (Ed.), Organic Reactions IV, Wiley, New York, 1948.
[44] R. Foster, J. Phys. Chem. 84 (1980) 2135–2141.
[45] J. Masnovi, E. Seddon, J. Kochi, Can. J. Chem. 62 (1984) 2552–2559.
[46] V. Kiselev, J. Miller, J. Am. Chem. Soc. 97 (1975) 4036–4039.
[47] W. Adam, A. Schonberger, Chem. Ber. 125 (1992) 2149–2153.
[48] L. Eberson, S. Shaik, J. Am. Chem. Soc. 112 (1990) 4484–4489.
[49] A. Klimkans, S. Larsson, J. Chem. Phys. 189 (1994) 25–31.

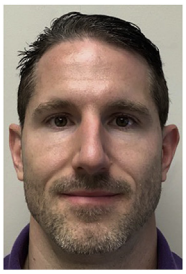

Joshua Halstead received his B.S. and M.S. degrees in chemistry from Cleveland State University in 2011 and 2013 respectively. He is employed in industry as a chemist for polymeric materials and coatings, working at such companies as Sherwin Williams and currently The Lubrizol Corporation. jhay2277@gmail.com

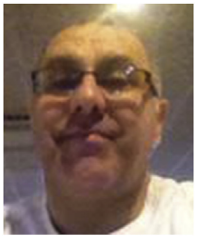

Refaat Abu-Saleh has worked in the education sector at the high-school level for 21 years and the college level for 11 years. He obtained a B.S. in Educational Chemistry from Edinboro University of Pennsylvania (1997), and a M.S. and Ph.D. in chemistry from Cleveland State University (2007, with J. Masnovi). His teaching includes courses ranging from elementary chemistry to organic chemistry. rabusale@kent.edu

Steven M. Schildcrout is Professor Emeritus of Chemistry at Youngstown State University. He retired in 2005 from teaching general and physical chemistry since 1969. He did his S.B. in chemistry (1964) at the University of Chicago and his Ph.D. in physical chemistry (1968, with F. E. Stafford) at Northwestern University. His postdoctoral work (1968–1969) was in J. L. Franklin's mass spectrometry group at Rice University. His research has included gaseous ion chemistry of organic and organometallic compounds and transition-metal complexes by mass spectrometry, chemical education, and computational molecular modelling. smschildcrout@ysu.edu

John Masnovi was Professor of Chemistry at Cleveland State University for 33 years until his recent death. He received both his B.S. in chemistry (1975) and M.S. in organic chemistry (1977) from Notre Dame University and his Ph.D. in organic chemistry (1982, with N. C. Yang) from the University of Chicago. He did a post-doctoral fellowship (1982–1985) in the research group of J. K. Kochi at Indiana University and the University of Houston. He taught organic chemistry at the undergraduate and graduate levels. He has published in organic, bioorganic, organometallic and electron-transfer chemistry.